LBL-19291 c.2

Lawrence Berkeley Laboratory
UNIVERSITY OF CALIFORNIA

Engineering Division

RECEIVED
LAWRENCE
BERKELEY LABORATORY
APR 7 1986
LIBRARY AND
DOCUMENTS SECTION

Presented at the IEEE Symposium on Timing Spectroscopy Short Course, Orlando, FL, October 30, 1984; and published in IEEE Transactions on Nuclear Science, NS-32, No. 3, June 1985, pp.1232-1241

NANOSECOND FLUORESCENCE SPECTROSCOPY

B. Leskovar

March 1985

TWO-WEEK LOAN COPY
This is a Library Circulating Copy which may be borrowed for two weeks.

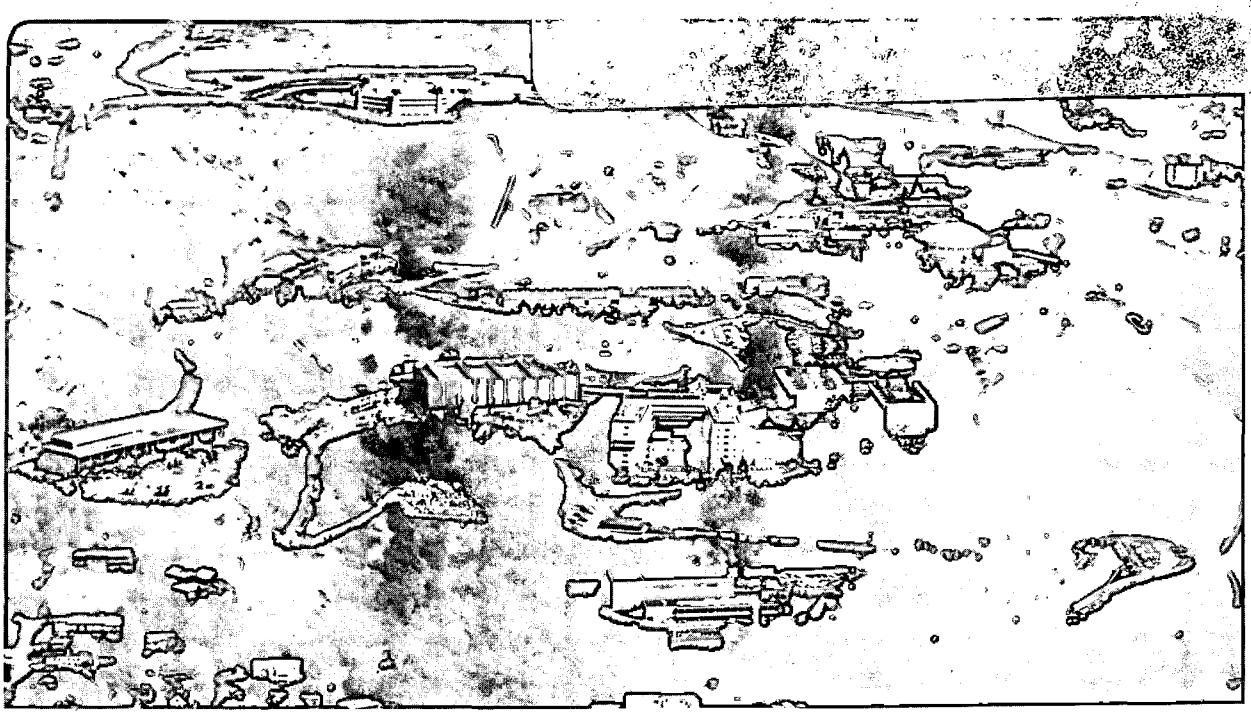

Prepared for the U.S. Department of Energy under Contract DE-AC03-76SF00098

LBL-19291 c.2

DISCLAIMER

This document was prepared as an account of work sponsored by the United States Government. While this document is believed to contain correct information, neither the United States Government nor any agency thereof, nor the Regents of the University of California, nor any of their employees, makes any warranty, express or implied, or assumes any legal responsibility for the accuracy, completeness, or usefulness of any information, apparatus, product, or process disclosed, or represents that its use would not infringe privately owned rights. Reference herein to any specific commercial product, process, or service by its trade name, trademark, manufacturer, or otherwise, does not necessarily constitute or imply its endorsement, recommendation, or favoring by the United States Government or any agency thereof, or the Regents of the University of California. The views and opinions of authors expressed herein do not necessarily state or reflect those of the United States Government or any agency thereof or the Regents of the University of California.

NANOSECOND FLUORESCENCE SPECTROSCOPY

LBL-19291

Branko Leskovar

Lawrence Berkeley Laboratory
University of California
Berkeley, California 94720 U.S.A.

ABSTRACT

This article is a summary of a short course lecture given in conjunction with the 1984 Nuclear Science Symposium. Measuring systems for nanosecond fluorescence spectroscopy using single-photon counting techniques are presented. These involve systems based on relaxation-type spark gap light pulser and synchronously pumped mode-locked dye lasers. Furthermore, typical characteristics and optimization of operating conditions of the critical components responsible for the system time resolution are discussed. A short comparison of the most important deconvolution methods for numerical analysis of experimental data is given particularly with respect to the signal-to-noise ratio of the fluorescence signal.

INTRODUCTION

Fluorescence spectroscopy is among the most sensitive and versatile technique available for studying the photophysical properties of organic molecules. The technique involves, directly or indirectly, the lifetime measurements of the excited molecular states. During the last sixteen years the method has proved to be extremely powerful and has added significantly to our understanding of the dynamic physical and chemical processes which are important in molecular biology. Fluorescence measurements permit a detailed analysis of macromolecules in solution or in organized structures with respect to their hydrodynamic properties (size and shape), polarity, dielectric strength, conformation, the binding characteristics of substrate and intermolecular or intramolecular distances and interactions. Particularly important are measurements of the changes in fluorescence parameters which occur with changes in temperature, pH factor, ionic strength, salt composition and other factors when molecules are in solutions.

Because the basic concepts of fluorescence spectroscopy have been reviewed elsewhere,[1,2] only a short summary will be given here.

When a molecule is excited by a light pulse to an upper singlet energy state, it rapidly goes to the lowest excited state without emission of light. There are several paths through which a molecule loses the acquired energy going from the lowest excited state to the rotational and vibrational level of the ground state. The molecule may emit the energy in the form of a photon to return to the ground state. If this occurs the process is called fluorescence. Molecules that tend to fluoresce are called chromophores. For most molecules emission occurs between 0.1 and 500 ns after excitation. There are other processes by which the molecule may return to the ground state without emission of fluorescence. In the process called radiationless deactivation the molecule loses the acquired energy slowly by collisions with surrounding molecules. Furthermore, in the nonradiative process called intersystem crossing, molecules may go to a metastable triplet state. From the triplet state the molecule can return to the ground state by a nonradiative or radiative (phosphorescence) process. Phosphorescence occurs longer after excitation than does fluorescence, in times ranging from a few microseconds to several seconds depending upon the molecule in question.

Another deactivation process from the excited state is through a photochemical reaction. The excitation energy is lost in rearranging bonds to form new products. Finally, a molecule can be deactivated transferring its energy to another neighboring chromophore by some coupling mechanism (energy transfer). The rate of each of these possible deactivation processes has been extensively treated in the literature.

For a given chromophore one of the most important deactivation processes is the fluorescence. It is experimentally characterized by fluorescence lifetime, spectrum, quantum yield and polarization. Only the measurement of the fluorescence lifetime will be considered in this paper.

Among the different techniques available for subnanosecond fluorescence lifetime measurements,[1,2] the single-photon counting method has gained wide acceptance. The sample is repeatedly excited with short light pulses and the resulting fluorescent pulses adjusted in intensity so that for most of the light flashes only one photoelectron is produced at the photocathode of a fast high-gain photomultiplier. The single photon counting technique of lifetime measurement is based upon the concept that the probability distribution for the emission of a single photon of fluorescence following a single exciting light pulse is identical to the intensity-time profile of the cascade of all the photons which are emitted following a single flash of exciting light. The single photon emission probability distribution is built up by repetitive exposure of the sample to short bursts of exciting light and recording of the time of arrival of the first photon of fluorescence following each exciting pulse. This is the most sensitive of techniques for measuring lifetimes, offering excellent signal-to-noise ratio, wide dynamic range of several decades of light intensity, and subnanosecond lifetime measurement capabilities. Due to the finite width of the light pulse, the time resolution limitations of the photomultiplier and the electronic signal processing system the experimental fluorescence lifetime curve is significantly distorted. In order to extract the true value of lifetime parameters from the experimental data, it is necessary to solve a convolution integral. Generally, the convolution procedure is more accurate if experimental data are measured under identical experimental conditions, particularly concerning the variations of photomultiplier and electronic circuitry parameters, as well as variations of the waveshape of the light pulse. Measurements have shown that in situations where a subnanosecond lifetime must be accurately measured, the fundamental limitations on the precision of measurements are due to the following factors:[3,4] the fluctuations in the light pulse waveshape, the single-photoelectron time spread of the photomultiplier, the dependence of the measuring system on the excitation and emission wavelengths and the timing error introduced by the discriminator or other circuit elements used in the system. Consequently, a high-precision measuring system should operate with the shortest possible exciting light pulses, because the time spread in the light pulse waveshape is in

absolute amounts smaller for narrower pulses. Also, the fastest photomultiplier with adequate gain operated under an optimized condition[5-8] must be used, since it will have a relatively smaller value of single-photoelectron time spread. To minimize the measuring system wavelength dependence, the same optical filter for the excitation light pulse is used in recording both the excitation and fluorescence emission time profiles. Also, the difference between excitation and fluorescence wavelength is chosen to be as small as practically possible.[3]

Over the past decade most single-photon counting measuring systems have employed as a light source either a relaxation-type spark gap light pulser or a synchronously pumped mode-locked dye laser. The relaxation-type light pulser systems[4] are generally simpler and considerably less expensive than the mode-locked laser based ones. They also offer wide spectral range from the vacuum UV to the near IR with adequate pulse width and intensity for most fluorescence experiments. However, a laser based system[9-13] has several important advantages. The excitation light pulse produced by a mode-locked laser is virtually a delta function, reducing considerably the measuring error due to the light pulse finite length and thus increasing the system resolution. Furthermore, the high light intensity and high repetition rate allows one to study samples having very small quantum yield and exceedingly small volume. In this paper we will describe both the spark gap and the mode-locked dye laser based systems.

Measuring System Based On The Relaxation Type Spark Gap Light Pulser

A block diagram of the photon counting system, based on an approach given in Ref. 4, is shown in Fig. 1. Basically, the system electronics can be divided into four main sections: the reference (START) channel, the fluorescence (STOP) channel, a data accumulation channel and a computer. More specifically, the system consists of a light pulser, a reference constant-fraction discriminator, a fluorescence signal constant-fraction discriminator with upper and lower level adjustments, a photomultiplier with its thermoelectric cooling chamber, delay lines, a time-to-pulse amplitude converter, a pulse-height analyzer, an analyzer-to-computer interface and a computer. All components used in the system are available commercially with the exception of the constant-fraction discriminator with upper and lower level adjustments, a component which significantly increases the accuracy of a measurement. The discriminator is described in considerable detail in Ref. 4.

In our experimental system, an Ortec 9452 nanosecond light pulser, with operating conditions adjusted to minimize the light pulse waveshape spread, was used as the light source. The light pulser operates as a relaxation oscillator and generates light pulses by a spark discharge between tungsten electrodes.

The sample was placed in the cuvette and repeatedly excited with nanosecond pulses of light. Colored glass or interference filters A and B are used to isolate the proper wavelength of excitation and fluorescence emission for each individual sample. The fluorescence light is detected at 90° to the exciting light. The lenses A and B (focal lengths 15 mm each), focus the exciting light onto the sample and fluorescence light onto the photomultiplier photocathode, respectively. Both lenses have a diameter of 25 mm. The fluorescence light is attenuated with the variable diaphragm to a low enough intensity so that the detection system is in the single-photoelectron mode. This mode is obtained when about 10% of the exciting light pulses result in an output pulse from the photomultiplier. The variable diaphragm aperture is typically 20 mm. The photomultipliers used were RCA 8850 or 8852. The former has a 116 spectral response, and the latter has a 119 ERMA III spectral response which extends into the near-infrared region.

The choice of photomultiplier for a particular experiment depends upon the wavelength of the fluorescent light. The photomultiplier should be placed in a thermoelectric cooling chamber to reduce the dark pulse counts. The reference (START) pulse was obtained from an RCA 1P28 photomultiplier, operating at 1.2 kV. It was optically coupled by means of a 12-in. long American Optical LG 3 light guide to the light pulser. The sample cuvette, the fluorescence and reference photomultipliers, the thermoelectric cooler, the interference filters, the diaphragm and the shutter are all mounted in a metal compartment that is light tight and electrical-interference tight. The aperture of the variable diaphragm was adjustable from outside of the compartment. The fluorescence signal photomultiplier output pulses were processed in a specially designed constant-fraction discriminator, with upper and lower level adjustments, which had a time walk less than ±35 ps over a 50 mV to 5 V input pulse amplitude variation. The constant-fraction discriminator output was applied to the STOP input of a time-to-pulse height converter through an adjustable delay line, when used for calibration purposes. The reference channel photomultiplier output pulse was processed in a constant-fraction discriminator to minimize time spread. The signal from the first output channel of the discriminator was applied to the START input of the time-to-pulse height converter through a second delay line. The signal from the second output channel of the reference channel discriminator was applied to the first input of a two-channel counter with a dual display. Whenever a pulse appeared at the STOP input of the time-to-pulse height converter, following a START pulse within a preset interval, an output pulse was produced at the first channel of the time-to-pulse height converter. This pulse was applied to the second channel of the dual counter and it was counted as a single photon event. Since the dual counter had a count preset capability from 10^2 to 10^7 counts, a direct percentage readout of the measuring system counting efficiency was readily available. The time-to-pulse height converter was followed by an analog-to-digital converter whose output pulses were applied to a 1024 channel pulse-height analyzer.

After many excitations, the number of counts vs. the channel number on the multichannel analyzer gives the decay time function of the fluorescence intensity. The relation between the channel number and time is established by calibrated variable delay lines. Since the analysis of fluorescence decay data requires corrections for the shape of the light pulse and the evaluation of the complex decay functions, the multichannel analyzer memory contents are transferred to a Sigma 2 computer for further numerical analysis. The multichannel analyzer is interfaced with the computer by means of the LBL analyzer-to-computer interface.

Nanosecond Light Pulser Considerations

A critical evaluation of the photon counting system shows that the spread in the light pulse waveshape is one of the fundamental limitations to the precision of the measurements. For an accurate measurement of fluorescence lifetimes and to reduce the required mathematical corrections, the spread in the light

pulse waveshape should be as small as possible compared with the sample decay time. This is particularly important in situations where operating conditions of the photomultipliers have been optimized to obtain a minimum value of the photomultiplier single-photoelectron time spread.[5,6]

For the relaxation-type nanosecond light pulser, such as Ortec Model 9352, which uses two tungsten electrodes to form a spark gap, measurements have shown that the optimum operating voltage for a minimum light pulse spread is 5 kV. In this case the full width at half maximum of the light pulse is less than 800 ps. The tungsten electrode spacing, which is adjustable between 0 and about 2 mm by means of a collar near the spark chamber,[4] should be adjusted to a light pulse rate of 14×10^3 pulses/s. Under these operating conditions, the photon yield will be approximately 2.8×10^6 photons/pulse. Also, to obtain stable performance of the light pulser both with respect to the light pulse intensity and waveshape spread, it is necessary to continually flush the spark gap chamber with a gentle flow of dry air during operation. The electrode tips have to be cleaned after every 10 hours of operation and the electrode spacing reset. Also it will be necessary to resharpen the electrodes into conical tips after significant erosion has occurred. The maximum photon yield of approximately 1.2×10^7 photons/pulse is obtained by using a nonoptimum operating voltage of 9 kV. Under these conditions, the FWHM of the light pulse is 2.2 ns, and the light pulse waveshape spread is about five times worse than in the case when the spark gap is operated with optimum operating voltage. Also, the light pulser performance is significantly degraded with increased air pressure in the spark chamber.

Filters

Colored glass or interference filters are used in the measuring system to isolate the proper wavelengths for excitation and to select the wanted fluorescence emission for each sample. Filters permit recordings with high collection efficiency and with a broad bandpass, which increases the system sensitivity. Glass filters also introduce significant fluorescence and phosphorescence artifacts into lifetime measurements. Exposure of certain colored glass filters to bright room lights may introduce phosphorescence emission which can be detected by the photomultiplier as an increase in the background count rate for over an hour after light exposure. In addition, the filters may capture a portion of scattered or incident exciting light and fluorescence photons and convert them into filter fluorescence arising in the glass. Filter fluorescence can add a low intensity (~0.5%) lifetime component to each spectrum taken. These system artifacts may have a significant effect on lifetime measurements, especially when the filter and sample lifetimes are very different.

Optimization of Photomultiplier Operating Conditions for a Minimum Transit Time Spread

The total electron transit time spread of the photomultiplier,[5,6] used in the subnanosecond photon counting system, represents the second major limitation on the precision of the decay time measurements. The transit time spread of an electrostatically focused photomultiplier consists of the photoelectron transit time spread between the photocathode and the first dynode of the multiplier, the electron transit time spread in the electron multiplier itself and that between the electron multiplier and the anode. The major causes of transit time spreads are the distribution of initial emission velocities of photoelectrons and secondary electrons, unequal electron path lengths between different electrodes, and nonuniform electric fields. Generally, the initial stages of a photomultiplier contribute predominantly to the total transit time spread. The transit time spread resulting from the initial velocity distribution is decreased by increasing the voltage between the photocathode and the first dynode. Similar considerations are valid for the secondary-electron initial velocity in an electron multiplier.

The single-photoelectron time spread and the time response of photomultipliers have improved considerably within the last few years due to better electro-optical design and to the application of new secondary emitters.

Optimization of operating conditions of the RCA 8850 and 8852 photomultipliers for a minimum transit time spread is performed by using the procedure and measuring system described in Ref. 5. For both types of photomultipliers, the single-photoelectron time spread has been measured as a function of the voltage ratio between the photocathode-focusing electrode and photocathode-first dynode, $(V_C-V_{FE})/(V_C-V_{D1})$, to determine the optimum operating conditions. The results of these measurements are given in Fig. 2 for full photocathode illumination. For the 8850 photomultiplier the transit time spread has a minimum value FWHM of 0.41 ns for $(V_C-V_{FF})/(V_C-V_{D1}) = 0.95$. The 8852 photomultiplier has a minimum time spread of 0.68 ns for $(V_C-V_{FE})/(V_C-V_{D1}) = 0.85$. The voltage-divider networks for both photomultipliers used in our system were designed according to the above criteria for a minimum time spread. Furthermore, positive voltage supplies were applied to the voltage-divider network in such a way that the photocathode was at the ground potential during operation. This voltage-divider configuration reduces the number of noise pulses generated by electroluminescence in the photomultiplier glass envelope and face plate because the thermoelectric cooling chamber components surrounding the photomultiplier are at ground potential.

Constant-Fraction Discriminator Considerations

The time resolution capabilities of the photon counting system, in addition to the spread in the light pulse waveshape and photomultiplier electron transit time spread, are determined by the time-walk and resolution characteristics of the constant-fraction discriminator. The discriminators used in this system were developed with improved time-walk and resolution characteristics. The photomultiplier signals are properly shaped by an attenuation-subtraction technique producing a pulse with a zero-crossing point and a pedestal added, allowing adjustment of the discriminator to the zero-crossing point. The fast baseline crossover point of a bipolar pulse is relatively independent of the pulse amplitude, and can be conveniently used to obtain amplitude-independent timing information. Despite the amplitude-independent crossover point of a bipolar pulse, a leading-edge detector triggered at this point introduces a time walk, in the nanosecond region, when there is a large dynamic range of input pulse amplitude. To overcome this shortcoming, a pedestal is added to shift the bias up to the detector threshold at the right time. By doing this, the detector triggers as soon as the zero-crossing point of the bipolar pulse is reached, producing an almost amplitude-independent timing pulse. To increase the input amplitude dynamic range of the discriminator, the bipolar pulse is further amplified and peak limited before being applied to zero-crossing

and threshold detectors. All essential functions responsible for time walk in the discriminator, such as threshold discrimination and fast pulse zero-crossing detection, are performed exclusively by tunnel diodes with a backward diode as nonlinear load. Other less essential functions, such as limiting, amplification, comparison and gain, are performed by hot carrier diodes, fast transistors and emitter-coupled logic elements, MECL III series.

To evaluate the performance of the constant-fraction discriminator, the system described in Ref. 5 was used to measure the time walk and resolution of the discriminator as a function of input pulse amplitude. Figure 3 shows the result of the measurement. The time walk of the discriminator is ±35 ps over an input pulse amplitude range from 50 mV to 5 V. The intrinsic time resolution of the discriminator with a constant 2 ns risetime pulse is 70 ps at 50 mV, decreasing exponentially to 20 ps at 800 mV.

Photon Counting System Wavelength Dependence Considerations

The presence of a significant wavelength dependence in the system response function can seriously limit the measurement accuracy, particularly when very short decay times are being measured. The system wavelength dependence arises in part in the photomultipliers, from the dependence of the kinetic energy of the emitted photoelectrons on the wavelength of the incident photons, and in part, in the light pulser emission profile wavelength dependence. The light pulser wavelength dependence can induce a spurious long decay time component in the analysis if the excitation and the fluorescence emission profiles are recorded at widely separated wavelengths. Concerning the light pulser wavelength dependence, it was observed that the red emission from the air gap spark discharge is broader in time and has a significantly longer tail component than the ultraviolet emission.[3] Generally, to minimize the system wavelength dependence, which may arise from both photomultiplier and light pulser effect, it is important to use the same light pulser-filter in recording both the excitation and fluorescence profiles and to minimize the difference between the excitation and fluorescence emission wavelengths.

Data Analysis

A number of theoretical approaches have been developed to extract the amplitude, α_i, and lifetime, τ_i, values from the experimentally determined excitation and fluorescence profiles. These approaches are discussed in more detail in the Numerical Analysis section of this paper. For the measuring system based on the relaxation-type spark gap light pulser the method of moments technique has been utilized for data analysis.

Results

Resolution characteristics of photon counting systems are measured with both a non-fluorescent scatterer and with erythrosin in water as the sample. In the first case, the sample is replaced by a piece of white reflecting surface at a angle of 45° to the symmetry axis of both the light pulser and the photomultiplier. The total system time resolution is expressed as the FWHM of the light pulse measured by a particular photomultiplier. With the RCA 8850 operated at the supply voltage of 3000 V and cooled down to 0°C, the system total time resolution was found to be 800 ps FWHM, as shown in Fig. 4. The spectrums are spaced 8 ns apart by means of a calibrated delay line and no colored filters were used. The spark gap was cleaned and adjusted before the measurement. The resolution decreases to approximately 1 ns in 30 hours of operating time if a gentle stream of dry air is used for flushing of the spark gap. Without dry air flushing, the resolution decreases to 1 ns in 15 hours of operating time.

The total system resolution is 1.48 ns when using the 8852 photomultiplier. The 8852 was operated with a supply voltage of 2800 V, applied only after the photomultiplier had been kept in the dark for 24 hours and cooled down to 0°C. During the measurements a Corning range glass filter, No. CS3-66, was used at the output window of the light pulser. The CS3-66 is a cutoff filter with a 0.02% transmittance at 540 nm and a 50% transmittance at 575 nm. The system resolution increases to 1.08 ns when a Corning CS5-58 blue glass filter is used instead of the CS3-66. The CS5-58 filter has transmittance of 0.02% at 340 and 480 nm, and a peak transmittance of 40% at 415 nm.

The system resolution and the short fluorescence lifetime measurement capabilities were determined by using erythrosin in water as the sample. Values of 57 ps, 90 ps and 110 ps have been reported for the lifetimes of erythrosin and erythrosin B (the disodium salt of erythrosin) in water. These measurements were obtained with a mode-locked laser system. In our measurement the sample of erythrosin (Eastman, Rochester, N.Y.) was purified by passing it through a silica gelmethanol column and suspended in a buffer solution of 40 mM Tricine-NaOH, 2 mM EDTA, pH 8.0. By using the 8850 photomultiplier and the light pulser with optimized operating conditions (light pulse waveshape is given in Fig. 5), as well as solving the convolution integral in order to extract lifetime parameters, the lifetime of this erythrosin solution was 90 ps for fluorescence emission at 550 nm that is excited at 490 nm, with a minor system artifact component of 4.7 ns, $[\alpha_2/(\alpha_1 + \alpha_2) = 0.04\%]$. The experimental and calculated lifetime curves are shown in Fig. 6. The noisy curve is the experimental fluorescence spectrum, the smooth curve is the calculated fluorescence response generated from the excitation profile best fit lifetimes and intensities: $\alpha_1 = 0.429$, $\tau_1 = 88$ ps, $\alpha_2 = 0.00017$, $\tau_2 = 4.71$ ns.

FLUORESCENCE MEASURING SYSTEM BASED ON SYNCHRONOUSLY PUMPED MODE-LOCKED DYE LASER

Although the single photon counting systems based on the spark gap light pulser are well suited to lifetime studies in the majority of applications, the lifetime measurements may become very difficult when the fluorescence intensities are too low due to low sample quantum yield, low chromophore concentration, and when the measured lifetimes are very short in comparison with the excitation pulse width. In such cases a mode-locked tunable dye laser is well suited as an excitation source for measurement of relaxation phenomena on subnanosecond time scale. In general, particular advantages of the pulsed dye laser source use are: very short excitation pulses having FWHM width of approximately 10 ps, high peak pulse power (in excess of 150 W at 590 nm), high pulse repetition rate, constant pulse waveshape over short and long decay time ranges, monochromatic and polarized excitation light and adjustability of the light wavelength. A block diagram of the single-photon counting system, based on descriptions given in Ref's. 10 and 12, using synchronously pumped mode-locked dye laser is shown in Fig. 7.

Measuring System Description

The major components of the measuring system are the pulsed laser light source, a reference fast photodetector, a fluorescence signal constant fraction discriminator, a photomultiplier with its cooling chamber, a rate reducer, delay lines, a time-to-amplitude converter, a pulse-height analyzer and a computer system.

The excitation light pulse in the single-photon counting system was provided by a Spectra Physics synchronously pumped, mode-locked dye laser. The pump laser was a Spectra Physics SP 171 argon ion laser which is acoustooptically mode-locked. The acousto-optic mode locking crystal was driven by a Spectra Physics SP 362 Ultrastable Mode Locker. The output pulses of the argon ion laser had a FWHM width of about 150 ps and a wavelength of 514 nm. The output of the argon ion laser was used to pump a modified Spectra Physics SP 375 dye laser. The dye laser cavity had been extended to match the cavity length of the argon ion laser. The modified dye laser produced light pulses of 10 ps, FWHM, at an 82 MHz repetition rate. The significant shortening of the dye laser pulse as compared to the argon ion laser pulse is due to a partial reduction of the pump-pulse induced population inversion by stimulated emission which is induced by simultaneous transit of the dye pulse through the dye stream.

Pulses with a FWHM as short as 1.5 ps at 620 nm can be obtained by using the laser dye rhodamine 6G, pumping at the threshold of lasing (about 750 mW argon laser pump power), and carefully matching the cavity lengths of the two lasers. For the fluorescence lifetime experiments, it was more convenient to run the dye laser above threshold and pump it with about 950 mW argon ion laser power.

The sample was placed in the cuvette and it is repeatedly excited with laser pulses. The interference filter D is used to isolate proper wavelength of fluorescence emission for each individual sample. The fluorescence light is detected at 90° to the exciting light. The lenses C and D focus the exciting light onto the sample and fluorescence light onto the photomultiplier photocathode, respectively. An RCA C31034A photomultiplier was used to detect the fluorescence photons. A fast photodiode, Texas Instrument TIED-55 picked up the excitation light pulses from the beam splitter, producing subnanosecond pulses at a repetition rate of 82 MHz. A tunnel diode leading edge discriminator shaped the photodiode output signal into a series of uniform 4 ns-wide standard Nuclear Instrument Modules pulses.

Conventional single-photon timing systems start a voltage ramp in the time-to-amplitude converter upon each excitation pulse and stop the voltage ramp when a fluorescence photon is detected. Because the 82 MHz repetition rate of the laser pulse is too high for the time-to-amplitude converter ramp on each pulse, a reverse single-photon timing scheme is used. The time-to-amplitude converter starts with the output of the constant fraction discriminator (fluorescence photon) and stops with the next pulse from the fast discriminator, i.e., with the next laser pulse. Since many excitation flashes do not produce fluorescence photoelectrons, the stop rate will be much higher than the fluorescence signal rate. This very high stop rate present at the converter input generally results in its poor performance. Apparently, the 82 MHz stop pulse train continuously present at the input of the converter interferes with the start input causing large oscillations in the measured fluorescence decay curve. To eliminate this high frequency crosstalk problem a rate reducer circuit was used. The rate reducer was placed between the discriminators and the time-to-amplitude converter. The rate reducer gates out all of the stop pulses that arrive before the arrival of the single-photon pulse from the constant fraction discriminator. Thus only one stop pulse is generated after each single-photon count. This practically eliminated oscillations in the fluorescence decay curve. The rate reducer circuit is described in detail in Ref. 12.

The proper timing of the inputs to the converter was adjusted by individual variable delay lines. The amplitude of the converter output can thus be made proportional to the time interval of the start-stop pulse pair at its inputs. The converter output was then processed by a Northern 1024 analog-to-digital converter and stored locally in a Northern NS646 multichannel analyzer. The contents of the multichannel analyzer are transferred to a VAX 11/780 computing system for data analysis.

Application of Pulsed Laser Photon Counting System

Pulsed laser photon counting system has been used extensively to study fluorescence decay kinetics in photosynthetic systems.[10] A typical result from spinach chloroplasts with reaction centers open in the presence of Mg^{+2} is shown in Fig. 8 at low excitation intensity (F_0 level). Fluorescence decay curve oscillation-free performance is possible only by using the rate reduction described above. By using the rate reduction of discriminator pulses reaching the time-to-amplitude converter the need of reducing the laser pulse rate with a cavity dumper is avoided.

In Fig. 8, E(t) is the excitation light waveshape (300 ps, FWHM), and F(t) is the measured fluorescence decay curve. The smooth three-exponential best fit is shown superimposed on the measured curve. The nonlinear least square method, described in the Numerical Analysis section of this paper, was utilized for data analysis. The lifetime (τ_1) and relative yield (ϕ_1) of the shortest component are 100 ps and 10%, respectively. This component was not resolved in previous single-photon fluorescence lifetime measurements.

The lower curves are the deviations between the best two- and three-exponential fits and the measured fluorescence data. A plot of the deviations between the best two-exponential fit and the data is plotted on a linear scale in the middle part of Fig. 8. The oscillating pattern near the peak value of the data is above the noise level and indicates that the decay cannot be described by two exponential functions. The lowest part of Fig. 8 shows that the deviations resulting from the best three-exponential fit contain only statistical noise. Consequently, the decay is properly described by three exponential functions. The random-noise character of the bottom deviation plot could not have been obtained even with a larger number of exponential decay components if system oscillations had been present in the measured fluorescence decay.

Based on deconvolutions of simulated data the pulsed laser single photon counting system can resolve fluorescence lifetimes as short as 25 ps. The limiting factors of the measuring system are the single photoelectron time spread of the photomultiplier, the timing errors introduced by electronics, the fluctuations in the light pulse waveshape and the measuring system dependence on the excitation and emission wavelengths. Application of a high gain microchannel plate or static crossed-field photomultiplier with an

appropriate infrared sensitive photocathode would increase the measuring system time resolution.[15,16]

Contemporary microchannel plate photomultipliers with protective films between their photocathodes and the input face of their first plate will have a very small single photoelectron time spread. Also they will have no afterpulses. In contrast, all conventionally designed high gain photon detectors with classical dynode structures for electron multiplications exhibit a certain amount of afterpulses after the main anode output pulse.[17,18] Afterpulses are produced as a result of the ionization of residual gases in the volume between the photocathode and the first dynode, as well as between the first several dynodes. The positive ions formed are accelerated toward photocathode by the focusing electric field or toward the first several dynodes. On impact these ions liberate secondary electrons which produce an afterpulse signal. In photon counting systems photomultiplier afterpulses can generate small amplitude late spurious peaks in the sample fluorescence decay profile. As a matter of fact, almost all published excitation and fluorescence decay profiles show secondary peaks of low intensity. The application of microchannel plate photomultipliers with protective film completely eliminates late spurious peaks from the fluorescence decay profile.

NUMERICAL ANALYSIS

The fluorescence lifetime determination involves measurements of both the response of measuring system, E(t), and the fluorescence decay curve, F(t). E(t) and F(t) are measured with a scattering solution and a fluorescent sample in the sample cell, respectively. If I(t) is the actual sample fluorescence decay that is sought in a lifetime experiment, F(t) is related to E(t) by the convolution integral:

$$F(t) = \int_0^t I(s)\, E(t-s)ds \qquad (1)$$

In general, the width of E(t) is not negligibly small in comparison with the width of F(t). Consequently, the actual sample fluorescence decay I(t) can be only obtained by a suitable convolution technique. Two more popular methods for numerical deconvolution of Eq. (1) are the method of moments[19] and the nonlinear least squares method.[20-22] In both methods one assumes that the fluorescence emission from a set of identical fluorophores in response to a delta pulse of exciting light is given by the relation:

$$I(t) = \sum_{i=1}^{N} \alpha_i \exp(-t/\tau_i) \qquad (2)$$

where N is the number of fluorescence components, and α_i and τ_i are the relative intensity and lifetime, respectively, of the ith component. The experimentor must determine the best fit values for α_i, τ_i and N for each sample investigated. This multiexponential form does cover a large number of cases of fluorescence decay. The fluorescence yield of the ith component is given by:

$$\phi_i = \alpha_i \tau_i \qquad (3)$$

It is equal to the number of photons emitted in the ith phase.

Method of Moments

In the method of moments for the extraction of the amplitude and lifetime values from the experimentally determined excitation and fluorescence decay profiles, one defines the moments by:

$$\mu_k = \int_0^\infty t^k F(t)dt \qquad (4)$$

and

$$m_k = \int_0^\infty t^k E(t)dt \qquad (5)$$

and a set of quantities G_w by:

$$G_w = \sum_{i=1}^{N} \alpha_i \tau_i^{\,w} \qquad (6)$$

It can be shown that:

$$\mu_0 = G_1 m_0,$$

$$\mu_1 = G_1 m_1 + G_2 m_0,$$

$$\frac{\mu_2}{2!} = G_1 \frac{m_2}{2!} + G_2 m_1 + G_3 m_0 ,$$

$$\vdots$$

$$\frac{\mu_k}{k!} = \sum_{w=1}^{k+1} G_s \frac{m_{k+1-w}}{(k+1-w)!} \qquad (7)$$

These are a set of equations that are linear in the parameter G_w. Given the moments of the excitation E(t) and the moments of fluorescence F(t), one can obtain G_1, G_2 ... from Eqs. (7). Furthermore, knowing G_1, G_2, ... G_{2N}, one can obtain the decay times, τ_1, τ_2, ...τ_N as the roots of the polynomial equation:

$$\begin{vmatrix} 1 & \tau & \tau^2 & \dots & \tau^N \\ G_1 & G_2 & G_3 & \dots & G_{N+1} \\ G_2 & G_3 & G_4 & \dots & G_{N+2} \\ \vdots & & & & \\ G_N & G_{N+1} & G_{N+2} & \dots & G_{2N} \end{vmatrix} = 0 \qquad (8)$$

From the known decay times τ_1, τ_2, ... one obtains the amplitudes α_1, α_2, ... from the following set of equations:

$$G_1 = \sum_{i=1}^{N} \alpha_i \tau_i ,$$

$$G_2 = \sum_{i=1}^{N} \alpha_i \tau_i^{\,2} ,$$

$$\vdots$$

$$G_N = \sum_{i=1}^{N} \alpha_i \tau_i^{\,N} . \qquad (9)$$

This procedure formally solves the problem of obtaining the amplitudes and decay time constants from the experimental data.

The method of moments has been widely used as a practical formalism for handling fluorescence data. A number of method modifications have been introduced in recent years to further enhance its usefulness. Specifically, the moment index displacement procedure was introduced for correction of the most common errors that exist in present day measuring systems. Furthermore, an introduction of the exponential depression procedure has reduced the cutoff error and increased the precision of data analysis. These modifications and others have been considered in considerable detail in Ref. 2.

Nonlinear Least Squares Method

The nonlinear least square method also has been widely used for numerical deconvolution. It is particularly suitable for deconvolution of multiexponential lifetime decay and other than exponential lifetime profile. Furthermore, the method can reliably deconvolute the sum of two or more exponentials when the lifetimes are quite close. However, in some cases it requires more complex programming algorithms than the method of moments resulting in slower computational speed of deconvolution, particularly when the signal-to-noise ratio of experimental data is low or when the instrumentation system has significant amounts of system artifacts. With high signal-to-noise ratio data and a small amount of artifacts both methods have approximately the same performance when fluorescence lifetime profile contains one or two exponential functions. When fits to three exponential functions are sought with a data signal-to-noise ratio larger than 10 and without significant system artifacts, experience reported in Ref. 10 suggests that the nonlinear least square method can achieve solutions faster than the method of moments and it is less likely to result in computer error when approaching the solution.

In the least squares method a nonlinear minimization routine is used to minimize the least square residual:

$$S = \sum_{j=1}^{ND} [F_j(t)-C_j(t)]^2/F_j(t) \qquad (10)$$

where ND is the number of data points and $F_j(t)$ and $C_j(t)$ are the jth points in the fluorescence data (after subtraction of the photomultiplier dark counts) and the calculated reconvolution using a particular set of α_i and τ_i, respectively. In the single photon counting case the signal-to-noise ratio is proportional to the square root of the number of counts. Therefore, the factor $1/F_j(t)$ weights the square deviation at the jth point by $1/\sigma^2$, where σ is the standard deviation of the jth point. The factor $1/F_j(t)$ is the appropriate weighting factor for a least square residual.[22]

Using an appropriate computing algorithm, the deconvolution by the least square method can be readily accomplished. Computer program called FLORFIT and its associated subroutines is mostly an implementation of the method described in Refs. 10 and 12. This program is capable of fitting a sample of fluorescence lifetime profiles which are not a sum of exponential functions. In this case the numerical procedure is much slower since it does not use the simplification that results when using exponential decay laws.

In addition to the moments and least square deconvolution methods, a number of other approaches have been developed to extract the amplitude and lifetime values from experimentally determined excitation and fluorescence profile. The best known are phase plane, Laplace and Fourier transform methods. They are described and compared in considerable detail in Ref. 2.

CONCLUSIONS

The objective of this paper is to provide a reasonably detailed overview of measuring systems for nanosecond fluorescence spectroscopy and to identify the most critical factors responsible for the system time resolution. Together with other papers given in this Short Course the author hopes that the reader will obtain a comprehensive picture of the whole field of fluorescence spectroscopy based on the single photon counting technique. Future improvements in this field will concentrate on development of new optoelectronic and electronics components, such as microchannel plate and static crossed field photomultipliers, with better time resolution capabilities than presently available. Furthermore, improvements are needed in the domain of deconvolution methods for numerical analysis of experimental data. This is particularly important in cases when samples that are small in size and have low fluorescence quantum yields are analyzed. Such samples generate fluorescence signals with a small value of the signal-to-noise ratio requiring a long signal processing time which result in reduced accuracy of numerical analysis. With improved measuring systems and refined deconvolution methods, it should be possible to determine fluorescence lifetimes as short as 10 ps.

ACKNOWLEDGEMENTS

This work was performed as part of the program of the Electronics Research and Development Group of the Department of Instrument Science and Engineering of the Lawrence Berkeley Laboratory and was supported by Lawrence Berkeley Laboratory and the U.S. Department of Energy under Contract No. DE-AC03-76SF00098. Reference to a company or product name does not imply approval or recommendation of the product by the University of California or the U. S. Department of Energy to the exclusion of others that may be suitable.

REFERENCES

1. J. Yguerabide, Nanosecond Fluorescence Spectroscopy of Macromolecules, Methods in Enzymology, C.H.W. Hirs and S.N. Timesheff, Eds., 26, 498-578, Academic Press, New York (1972).

2. Time-Resolved Fluorescence Spectroscopy in Biochemistry and Biology, R.B. Cundall and R.E. Dale, Eds., Plenum Press, New York (1983).

3. P.R. Hartig, K.H. Sauer, C.C. Lo and B. Leskovar, Measurement of Very Short Fluorescence Lifetimes by Single Photon Counting, Rev. Sci. Instr., 47, No. 9, 1122-1129 (1976).

4. B. Leskovar, C.C. Lo, P.R. Hartig and K.H. Sauer, Photon Counting System for Subnanosecond Fluorescence Lifetime Measurements, Rev. Sci. Instr., 47, No. 9, 1113-1121 (1976).

5. B. Leskovar and C.C. Lo, Single Photoelectron Time Spread Measurement of Fast Photomultipliers, Nucl. Inst. Meth., 123, No. 1, 145-160 (1975).

6. B. Leskovar, Accuracy of Single Photoelectron Time Spread Measurement of Fast Photomultipliers, Nucl. Inst. Meth., 128, 115-119 (1975).

7. B. Leskovar, Time Resolution Performance Studies of High-Speed Photon Detectors, Proc. of the 4th International Congress, Laser 79-Optoelectronics, Munich, West Germany, 581-586. Pub. by IPC Science and Technology Press Ltd., England (1979).

8. B. Leskovar, Recent Advances in High-Speed Photon Detectors, Proc. of the 6th International Congress, Laser 83-Optoelectronics, Munich, West Germany, 68-74. Pub. by Springer Verlag: Optoelectronics in Engineering (1984).

9. V.J. Koester and R.M. Dowben, Subnanosecond Single Photon Counting Fluorescence Spectroscopy Using Synchronously Pumped Tunable Dye Laser Excitation, Rev. Sci. Instr., 49, No. 8, 1185-1191 (1978).

10. J.A. Nairn, Orientation and Energy Transfer Studies on Chlorophyll in the Photosynthetic Membrane, Doctoral Thesis, University of California, Berkeley, LBL Report LBL-13827 (1981).

11. H.E. Zimmerman, J.H. Penn and C.W. Carpenter, Evaluation of Single-Photon Counting Measurements of Excited-State Lifetimes, Proc. Nat'l. Acad. Sci., U.S.A., 79, 2128-2132 (1982).

12. B. Turko, J.A. Nairm and K. Sauer, Single Photon Timing System for Picosecond Fluorescence Lifetime Measurements, Rev. Sci. Instr., 54, No. 1, 118-120 (1983).

13. W.R. Ware, M. Pratinidhi and R.K. Bauer, Performance Characteristics of a Small Side-Window Photomultiplier in Laser Single-Photon Fluorescence Decay Measurements, Rev. Sci. Instr., 54, No. 9, 1148-1156 (1983).

14. Ortec Incorporated, Model 9352 Nanosecond Light Pulser, Operating and Service Manual (1972).

15. B. Leskovar and C.C. Lo, Studies of Prototype High-Gain Microchannel Plate Photomultipliers, IEEE Trans. Nucl. Sci., NS-26, No. 1, 388-394 (1979).

16. C.C. Lo and B. Leskovar, Performance Studies of High-Gain Photomultiplier Having Z-Configuration of Microchannel Plates, IEEE Trans. Nucl. Sci., NS-28, No. 1, 698-704 (1981).

17. C.C. Lo and B. Leskovar, Afterpulse Time Spectrum Measurement of RCA 8850 Photomultiplier, IEEE Trans. Nucl. Sci., NS-30, No. 1, 445-450 (1983).

18. B. Leskovar, The Afterpulse Time Spectra of High-Speed Photon Detectors, LBL Report LBL-18909 (1985).

19. I. Isenberg, R.D. Dyson and R. Hanson, Studies of the Analysis of Fluorescence Decay Data by the Method of Moments, Biophysical J., 13, No. 10, 1090-1115 (1973).

20. D.W. Marquardt, An Algorithm for Least-Squares Estimation of Nonlinear Parameters, J. Soc. Indus. Appl. Math., 11, No. 2, 431-441 (1963).

21. W.R. Ware, L.J. Doement and T.L. Nemzak, Deconvolution of Fluorescence and Phosphorescence Decay Curves. A Least-Squares Method, J. Phys. Chem., 77, No. 17, 2038-2047 (1973).

22. A. Grinvald and T.Z. Steinberg, On the Analysis of Fluorescence Decay Kinetics by the Method of Least-Squares, Anal. Biochem., 59, 583-598 (1974).

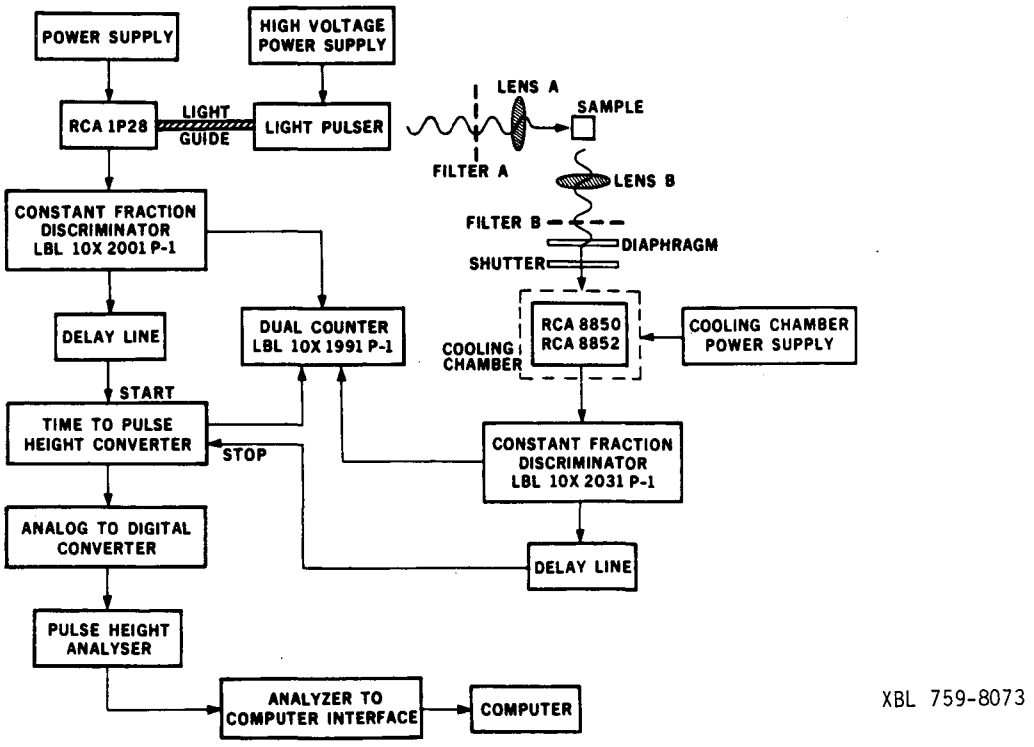

Fig. 1 Block diagram of the photon counting system for subnanosecond fluorescence lifetime measurements using relaxation-type spark gap light pulses.

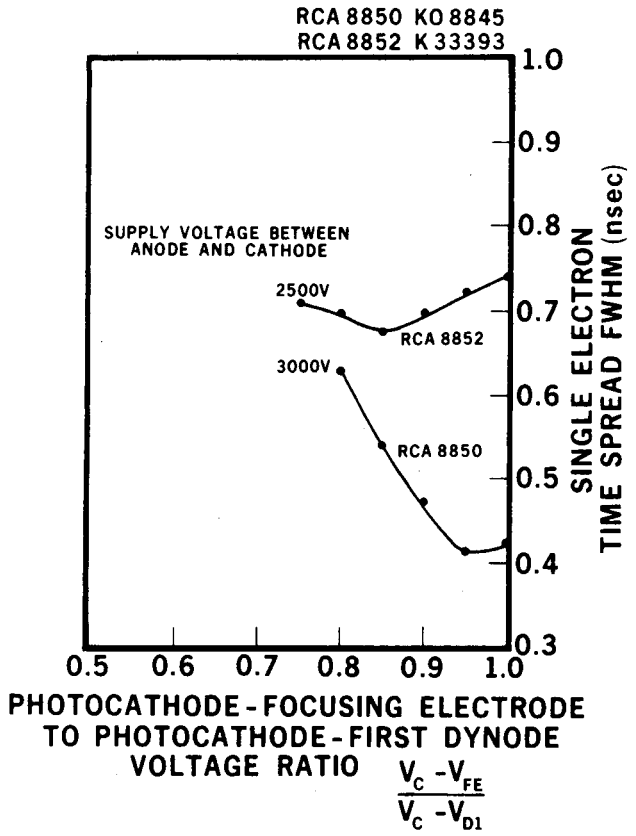

XBL 759-8074

Fig. 2 Single-electron time spread as a function of the voltage ratio between the photocathode-focusing electrode and photocathode-first dynode for the RCA 8852 and 8850 photomultiplier with full photocathode illumination.

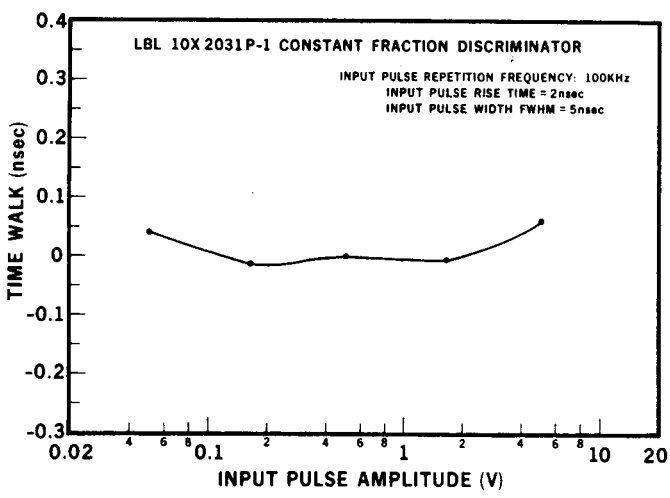

XBL 759-8075

Fig. 3 Time-walk characteristics of the constant-fraction discriminator as a function of the amplitude of the input pulse.

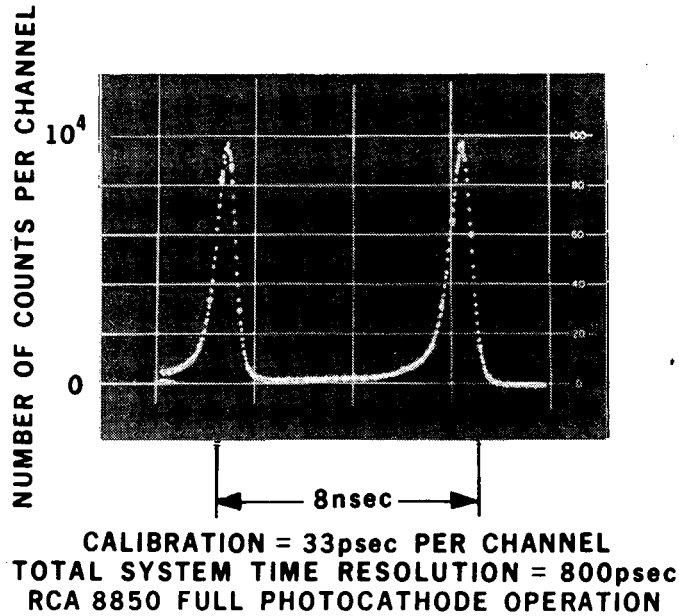

XBB 759-6534

Fig. 4 Measuring system total time resolution by using the RCA 8850 with full photocathode illumination as the photon detector.

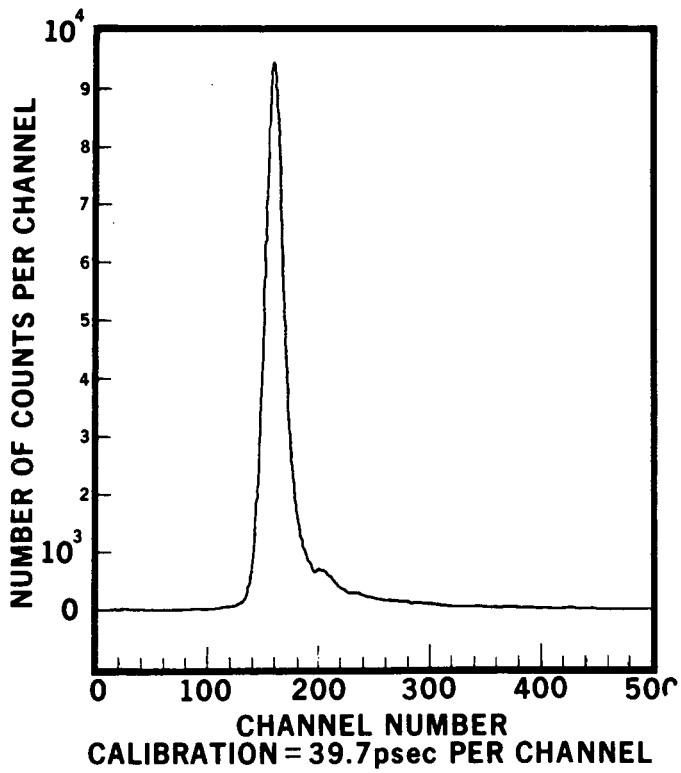

XBL 7512-9877

Fig. 5 Light pulse waveshape from the nanosecond light pulser with optimized operating conditions.

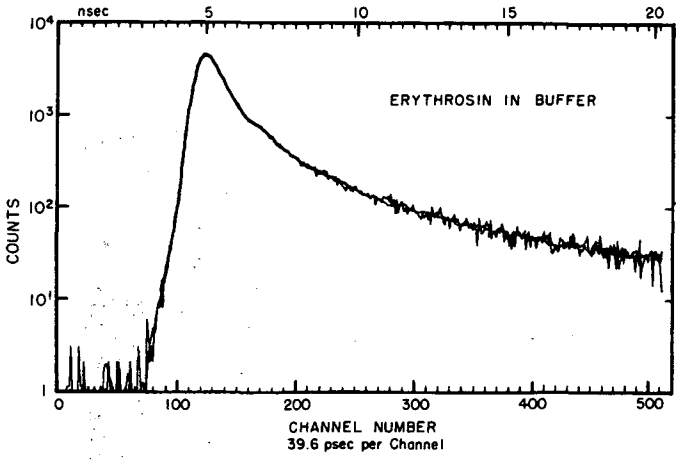

XBL 7510-4279

Fig. 6 Fluorescence of erythrosin (2.8×10^{-5} M) in 40 mM Tricine-NaOH, 2 mN EDTA pH 8.0.

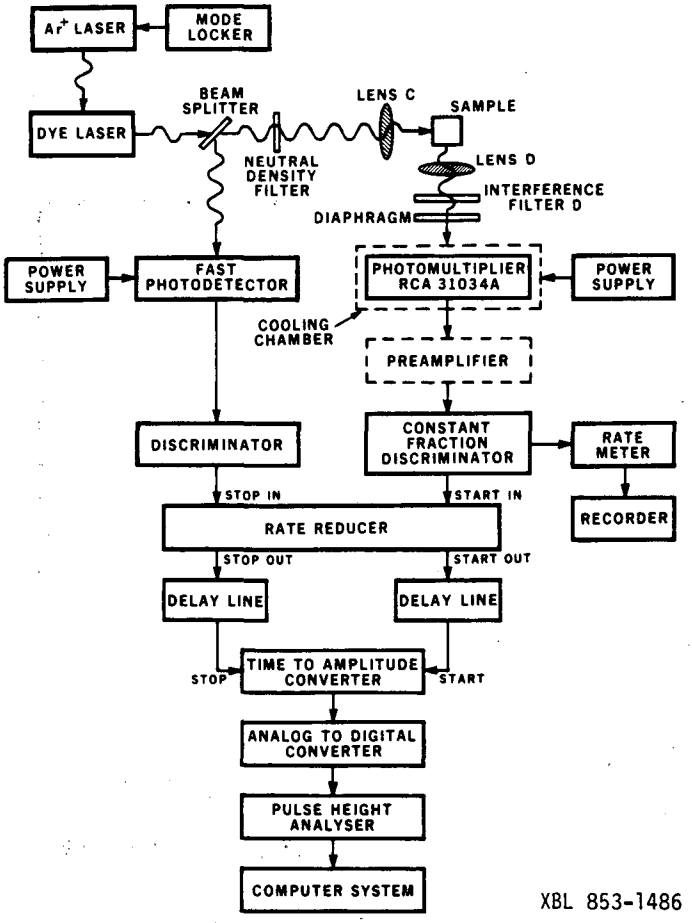

XBL 853-1486

Fig. 7 Block diagram of the photon counting system using synchronously pumped mode-locked dye laser.

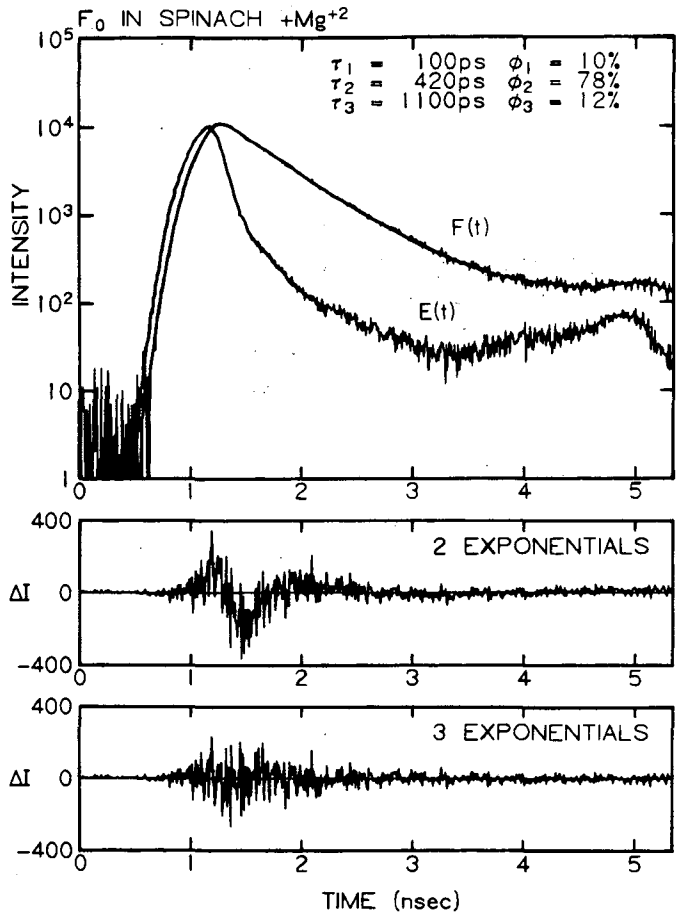

XBL 811-4430

Fig. 8 Typical experimental fluorescence decay data (of spinach chloroplasts) measured by the pulsed laser photon counting system.

This report was done with support from the Department of Energy. Any conclusions or opinions expressed in this report represent solely those of the author(s) and not necessarily those of The Regents of the University of California, the Lawrence Berkeley Laboratory or the Department of Energy.

Reference to a company or product name does not imply approval or recommendation of the product by the University of California or the U.S. Department of Energy to the exclusion of others that may be suitable.

LAWRENCE BERKELEY LABORATORY
TECHNICAL INFORMATION DEPARTMENT
UNIVERSITY OF CALIFORNIA
BERKELEY, CALIFORNIA 94720